RESEARCH PAPER



Estimation of Cerchar Abrasivity Index Using Petrographical, Textural and Mechanical Rock characteristics in Igneous Rocks

Seyed Sajjad Karrari ¹ ⁽¹⁾, Mojtaba Heidari ^{1,*} ⁽¹⁾, Jafar Khademi Hamidi ² ⁽¹⁾, Mohammad Khaleghi-Esfahani ³, Ebrahim Sharifi Teshnizi ⁴ ⁽¹⁾

Received: 08 February 2025, Revised: 28 April 2025, Accepted: 09 May 2025

Abstract

Cerchar Abrasivity Index (CAI) test is commonly used to assess the abrasiveness of rocks due to its efficiency and simplicity. This research focuses on estimating CAI values based on the petrographical, textural, and mechanical characteristics of igneous rock. The study examines the potential correlation between CAI values, petrographical, and textural characteristics using a dataset comprising 15 samples from 5 different types of igneous rocks. The researchers employed a range of statistical analyses, including Pearson's correlations, Simple and Multiple linear and non-linear regression, and artificial neural network (ANN) analyses. These methods were used to examine the relationship between CAI values and various parameters. CAI has a direct correlation with Texture Coefficient (TC), Heterogeneity (H), Saturation Index (SI), Uniaxial Compressive Strength (UCS), Abrasivity Index (ABI), and Rock Abrasivity Index (RAI), with the exception of Feldspathic Index (FI) and Porosity (P). Results showed that by increasing CAI values, the TC, H, RAI, ABI, and SI increased, and FI decreased. By increasing TC and H, the percentage of quartz increases, and alkali feldspar decreases. The study suggests SI, FI, TC, and H are appropriate in assessing the abrasiveness of igneous rocks. Validation of the results displayed that new models can be used for predicting CAI with acceptable accuracy.

Keywords: Cerchar Abrasivity Index, Petrographic Characteristics, Textural Coefficient, Heterogeneity, Igneous Rocks.

Introduction

In construction and mining projects, rock excavation can be carried out using traditional drilling and blasting methods or mechanical excavators. However, one challenge encountered during the excavation process is the varying strength and geomechanical properties of the rock surfaces, which significantly reduces the effectiveness of cutting tools. As a result, a significant portion of the excavation budget needs to be allocated towards repairing or replacing these rock cutting tools (Hamzaban et al. 2014; Lin et al. 2020). Sliding on the rock surface can cause degradation of the cutting tools used in excavation. The abrasiveness of the rock is influenced by various features, including the average quartz grain size, quartz, and abrasive mineral content, type of cement present, and degree of cementation (Yarali et al., 2008). These factors play a role in determining the rock's abrasiveness and can contribute to the wear and

¹ Department of Geology, Faculty of Sciences, Bu-Ali Sina University, Hamedan, Iran

² Department of Mining Engineering, Faculty of Engineering, Tarbiat Modares University, Tehran, Iran

³ Département de géologie et de génie géologique, Faculté des sciences et de génie, Université Laval, Québec, Canada

⁴ Department of Geology, Faculty of Sciences, Ferdowsi University, Mashhad, Iran

^{*} Corresponding author e-mail: moj.heidari@basu.ac.ir

deterioration of cutting tools during the excavation process.

Methods for determining the abrasiveness of rocks can be classified into two categories: petrological and mechanical tests. (West, 1981). Petrological tests involve examining the mineral composition, grain size, texture, and cementation of the rock. Mechanical tests, on the other hand, focus on assessing the physical and mechanical properties that influence abrasiveness. In recent decades mechanical tests such as the LCPC test, NTNU test, the Cerchar test, Cerchar hardness index (CHI), and petrological parameters including rock abrasiveness index (RAI), Schimazek's value (Sch), and petrographic studies were used to evaluate the rock abrasion (Yarali et al., 2008; Yarali, 2017; Balani et al., 2017; Majeed & Abu Bakar, 2015; Aydin, 2019). The Cerchar test is commonly employed in civil projects to assess rock abrasiveness. However, to establish a better understanding of its correlation with geomechanical properties, further investigations are necessary. Several researchers have proposed relationships between the Cerchar Abrasivity Index (CAI) and various petrographical, physical, and mechanical characteristics of rocks (Ko et al., 2016; Undul & Er, 2017; Aligholi et al., 2018; Yagiz et al., 2020; Shi et al., 2024). These relationships can provide valuable insights into the abrasiveness of rocks. The potential relationships between CAI and rock characteristics showed in Table 1.

The CAI test offers advantages in terms of its ease, affordability, and time efficiency. As a result, it is more commonly utilized for assessing rock abrasiveness compared to other methods like NTNU and LCPC (Aydin, 2019; Yagiz et al., 2020; Massalov et al., 2020). The CAI test method has been employed by using the British coal mining and is applied in the tunneling engineering as well (Karrari et al., 2023; Karrari et al., 2024). The CAI test is developed according to the French standard (AFNOR, 2000). ISRM has proposed a new method (ISRM-SM) to carry out this test.

Table 1. Relationships between CAI and rock characteristics

Scholars	Correlation with CAI	Rock type
(Er and Tugrul 2016)	CAI = 2.12 + 0.03 Wa	Granitic Rocks
	CAI = 1.87 + 0.04 SH	
	CAI = 2.55 + 0.58 Vp	
	CAI= 4.52+1.47 Qs	
	CAI= 2.73+0.04 SHV	
	CAI= 3.19+0.02 UCS	
	CAI= 3.73+0.11 BTS	
(Ko et al. 2016)	$CAI = 4.8668 + 0.05467 \ UCS - 0.149 \ B_1 - 0.2945 \ B_3$	Granite, Pegmatite, Propylite, Diorite, Gabbro
	CAI = -1.102 POPA + 3.850	Andesite and Rhyodacite
	CAI = 1.1265 (POPA)2 - 3.0879 (POPA) + 4.6078	
	CAI = -1.006 PPlg.Felds + 4.4504	
	$CAI = -0.4753 (PPlg.Felds)^2 + 0.3459 PPlg.Felds +$	
	3.6317	
	$CAI = 11.045(FOPA)^2 - 10.578(FOPA) + 5.0484$	
(Garzón-Roca and Torrijo 2020)	$CAI = 1.37CAI^* + 1.88$	Andesitic Rocks
(Torrijo Garzón-Roca 2020)	CAI = 1.8243 PL (mm) + 0.4447	Andesitic rocks
•	CAI = 0.0305 PL (%) + 0.6360	
	CAI = 0.055SiO2 + 0.026FeO + 0.055MgO	
	+0.024CaO $+0.022$ Na2O $+0.022$ K2O -1.32	

Wa: Waveness average, SH: shore harness, Vp: P-wave velocity, Qs: quartz size, SHV: Schmidt hardness value, BTS: Brazilian tensile strength, UCS: Uniaxial compressive strength, B_1 : Brittleness value ($B_1 = UCS / BTS$) B_3 : Brittleness value ($B_3 = UCS * BTS / 2$), POPA: Perimeter of opaque minerals, PPlg.Feld: Perimeter of plagioclase feldspar, FOPA: Feret's diameter of opaque minerals, PL (mm): Plagioclase grain size, PL (%): Plagioclase percentage, (SiO2, FeO, MgO, CaO, Na2O, and K2O percentage).

The CAI test consists of scratching a steel stylus by the hardness of (HRC 55 ± 1) with a 90° conical tip (Alber et al., 2014). In this study, according to the ISRM-SM, five tests are carried out on each sample to obtain the average CAI value. The scratching action's speed (accepted by ISRM-SM standard) is 10 mm/s for the CAI test.

Petrological, textural, and mechanical rock parameters are useful for obtaining the rock's abrasiveness. These factors have been employed by researchers to measure and evaluate the abrasiveness of rocks (Undul & Er, 2017; Yagiz et al., 2020; Teymen, 2020). In the following, recent studies that used petrographic, textural, and mechanical characteristics to evaluate the CAI are presented.

In the study conducted by Er & Tugrul (2016), empirical relationships were established between mineralogical, chemical, petrographical, and physicomechanical properties of different granitic rocks and the Cerchar Abrasivity Index (CAI). The results indicated that there was a positive correlation between the size and content of quartz grains in the granitic rocks and the CAI. This means that as the size and content of quartz grains increased, the CAI also increased, suggesting a higher level of abrasiveness. However, no significant relationship was observed between CAI and other minerals present in the granitic rocks, indicating that the quartz grains played a more dominant role in determining the rock's abrasiveness in this particular study. The influence of geomechanical characteristics on Cerchar abrasivity index in igneous and metamorphic rocks investigated by Ko et al., (2016). The result of multiple regression analysis shows that quartz mineral is not as important as UCS and brittleness index (B₃) to estimate the CAI values in igneous rocks. Previous scholars ignored the effect of textural properties on CAI value (e.g., Er & Tugrul, 2016; Ko et al., 2016). Because textural properties could show the effect of various minerals, it would be useful to evaluate its possible impact. Undul & Er (2017) studied the effect of texture and geo-mechanical characteristics on the abrasiveness of 23 igneous rocks (Andesite and Rhyodacite). The outcomes of physical and mechanical tests showed that as P-wave velocity, UCS, Brittleness index (B₃), BTS, and E increased, the CAI values increased as well. According to their study, increasing opaque minerals and grain sizes of altered plagioclase can decrease the CAI values. Aligholi et al. (2018) predicted the engineering characteristics of igneous rocks by using petrographic analysis. Their research shows that fine grained (0.08 - 0.15 mm) igneous rocks have better geomechanical properties (porosity, dry unit weight, P-wave velocity, I_{S50}, and less abrasiveness (CAI) in comparison with the coarse grained (0.30-1 mm) ones.

The primary objective of this research is to estimate CAI values using petrographical, textural, and mechanical rock characteristics. This approach helps to reduce the costs associated with sample preparation and transportation, as well as the time required for conducting laboratory experiments. On the other hand, petrographical studies can be conducted using smaller samples and basic laboratory equipment that is readily available. However, not all laboratories may have the specific equipment required for the CAI test. As a result, empirical analyses have been developed to estimate CAI values based on the petrographical characteristics of rocks, providing an alternative approach in cases where the necessary equipment is not accessible. Regression and ANN analyses are commonly applied in engineering studies and confirmed to be effective in relating CAI with geomechanical features (e.g., Majeed & Abu Bakar, 2015; Teymen, 2020; Garzón-Roca et al., 2020; Torrijo Garzón-Roca et al., 2020; Yagiz et al., 2020). Simple regression, multiple linear and non-linear regression, and ANN models are used in this research.

Methods

Sampling and geomechanical laboratory tests

For this research, a total of 15 samples were collected from seven sectors along the tunnel route

in the Gelas water transfer project in west Azerbaijan (Naghadeh City) of Iran (Fig. 1). 15 rock samples block from Adit (1500, 1550, 1600, and 1650) and cylindrical cores (BH12, KST22, KST23-S4-19 m, KST23-S5-268m, KST23-S6-206m, KST16, KSC1-45m, KSC1-82m, and KSA2) have been analyzed in this study. The photo of cylindrical core rock samples is shown in Figure 2. The selection of samples from various sectors allows for a broader representation of the geological conditions along the tunnel route, providing a more comprehensive understanding of the rock characteristics and their abrasiveness. The objective is to obtain CAI, petrographical, textural, and mechanical rock characteristics for estimating wear disc cutters of TBM. The wear disc cutter numbers will be obtained in the project in the future.

The sampling procedure followed the guidelines outlined in the ISRM 2007 guidelines. The collected samples included both slightly weathered and unweathered rock specimens. Special care was taken to ensure that the rock block samples were homogeneous and free from any weakness planes that could affect the test results. The cylindrical cores and rock blocks were obtained using a drilling process with a diameter of 54.7 millimeters. Rock core samples are prepared according to the ISRM (2007) standard. The porosity, unit weight, BTS, UCS, and point load strength (I_{S50}) tests were done based on ISRM (2007). In addition, the CAI test was performed based on ISRM (Alber et al., 2014). The list of test names, number of tests, and used standards are indicated in Table 2.

Table 2. The list of test names, number of tests and used standard

Test name	Number of tests	Used standard		
Porosity	5	ISRM (2007)		
Unit weight	5	ISRM (2007)		
BTS	10	ISRM (2007)		
UCS	5	ISRM (2007)		
I_{S50}	10	ISRM (2007)		
CAI	5	ISRM (2014).		

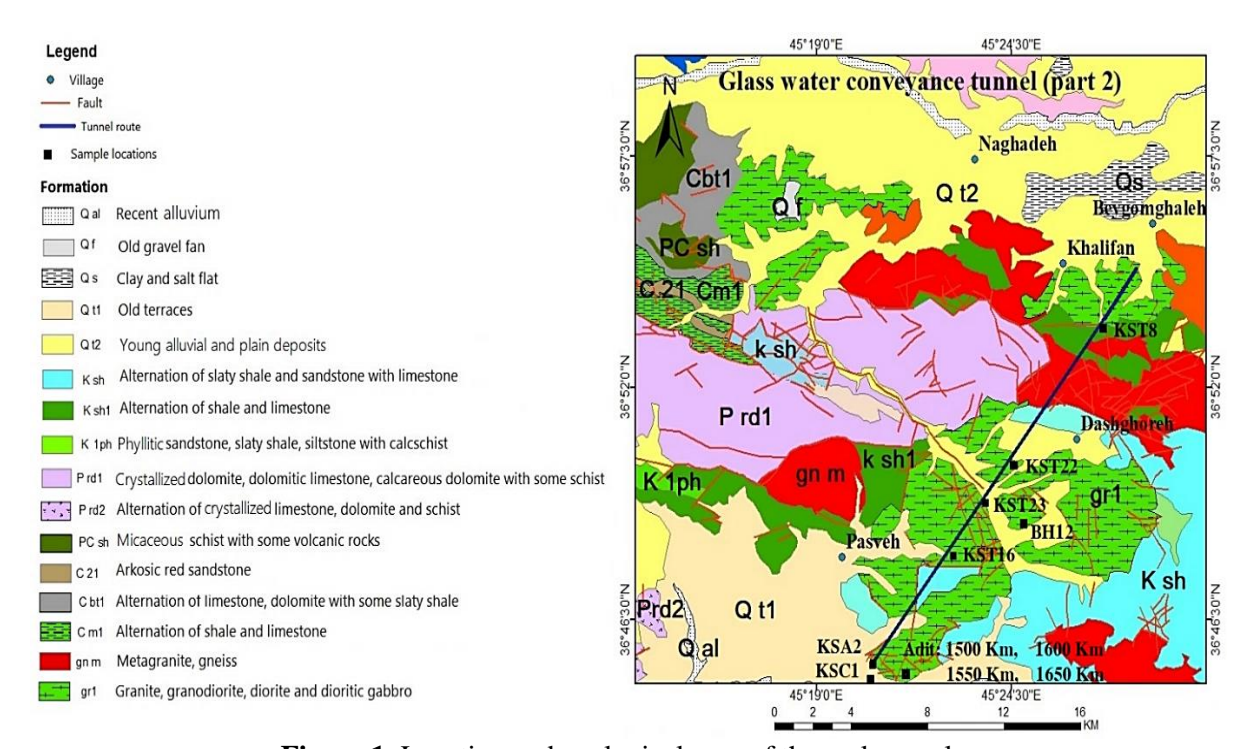


Figure 1. Location and geological map of the rock samples



Figure 2. The picture of cylindrical cores rock samples

In this study, various statistical analyses were conducted to investigate the relationships between the Cerchar Abrasivity Index, petrographic and textural features, and engineering properties of the rocks. These analyses included Pearson's correlation, simple regression, multiple linear regression, non-linear regression, and artificial neural network (ANN) analysis. These statistical techniques were employed to identify and quantify the relations between CAI values and the examined rock characteristics. By utilizing these analytical approaches, the study aimed to establish meaningful relationships and gain insights into how the petrographic and textural features of the rocks influence their CAI values and engineering properties. The statistical analysis was performed utilizing SPSS software version 23. Also, the ANN analysis was performed utilizing Matlab software version R2016a.

Cerchar abrasivity test

The CAI tests in this study were performed using the third-generation device developed by West (1989). A total of fifty-five HRC styluses were utilized for the testing process. The rock samples were securely held in a vise under a 7-kilogram load, and the surface was scratched at regular 10-millimeter intervals, as illustrated in (Fig. 3). The specimens had a diameter of 54 millimeters, a height ranging from 30 to 50 millimeters, and a smooth surface achieved through saw cutting. To ensure accurate and reliable results, this technique was carried out a minimum of five times in two directions using a new or resharpened steel tip for each individual sample.

Petrographic studies of rock samples

For the petrographic analysis, thin sections of the rock samples were studied using optical microscopy (Table 3). Thin sections are indicated for petrographic analysis in Figure 4. The major minerals, including quartz, plagioclase, and alkali feldspar, were classified according to the Streckeisen diagram of petrographical classification, following the standards set by the International Union of Geological Sciences (Streckeisen, 1976).

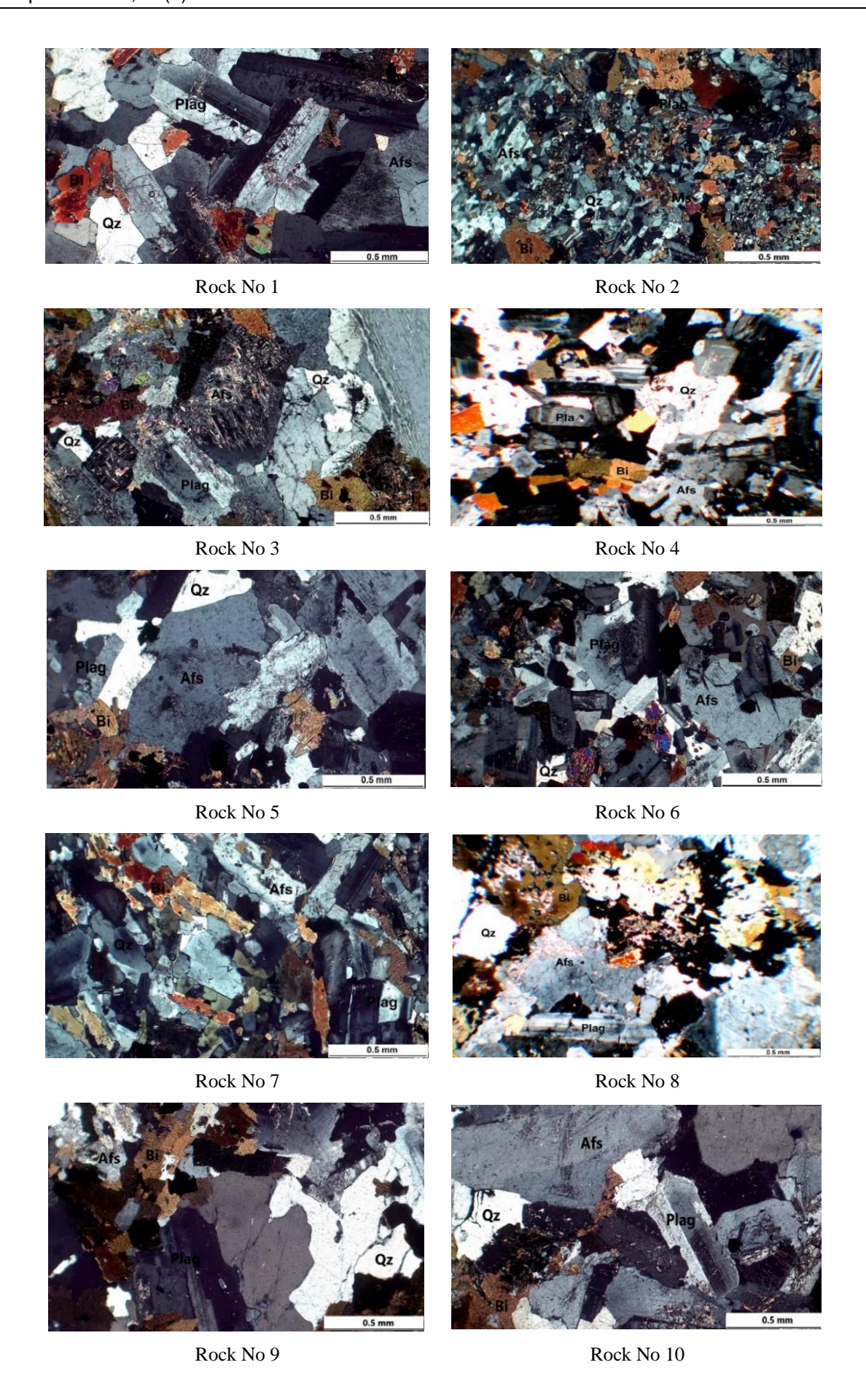
Table 3. Modal analysis, locations, and petrographic names of the studied rocks

Rock No	Location	Mineralogy (%)	Petrographic name
1	KSC1-82m	Alf: 42.65, Pl: 28.46, Qz: 18.43, Mos: -, Bio: 6.33, Chl: 3.00, Opa: 0.13, Amp: 1.00	Monzogranite
2	KST23-S5-268m	Alf: 30.72, Pl: 14.30, Qz: 12.70, Mos: 12.13, Bio: 32.47, Chl: 1.00, Opa: 1.44, Amp: 1.50	Syenogranite
3	KSa2	Alf: 38.38, Pl: 30.75, Qz: 12.73, Mos: -, Bio: 15.10, Chl: 1.50, Opa: 0.06, Amp: 1.50	Quartz monzonite
4	KST22	Alf: 50.21, Pl: 26.96, Qz: 6.97, Mos: -, Bio: 9.83, Chl: 5.00, Opa: 0.25, Amp: 1.00	Quartz syenite
5	KST16	Alf: 42.85, Pl: 15.36, Qz: 12.81, Mos: -, Bio: 15.68, Chl: 1.00, Opa: 1.41, Amp: 2.00	Syenogranite
6	KST16	Alf: 52.43, Pl: 13.88, Qz: 11.52, Mos: 2.13, Bio: 16.85, Chl: 1.00, Opa: 0.36, Amp: 2.20	Syenogranite
7	BH12	Alf: 50.92, Pl: 10.96, Qz: 9.97, Mos: - , Bio: 20.61, Chl: 4.50, Opa: 0.59, Amp: 2.60	Quartz syenite
8	BH12	Alf: 42.85, Pl: 11.32, Qz: 15.03, Mos: 1.29, Bio: 12.96, Chl: 2.00, Opa: 9.50, Amp: 2.50,	Syenogranite
9	1500 km	Alf: 42.76, Pl: 14.36, Qz: 26.88, Mos: -, Bio: 11.33, Chl: 4.00, Opa: 0.80, Amp: -,	Syenogranite
10	1550 km	Alf: 36.94, Pl: 19.37, Qz: 25.30, Bio: 14.26, Mos: -, Chl: 2.25, Opa: 0.13, Amp: 1.75,	Monzogranite
11	1600 km	Alf: 52.75, Pl: 10.84, Qz: 23.93, Mos: -, Bio: 6.39, Chl: 4.00, Opa: 0.06, Amp: 3.00	Syenogranite
12	1650 km	Alf: 46.54, Pl: 23.57, Qz: 21.23, Mos: 1.00, Bio: 7.07, Chl: 0.50, Opa: - , Amp: 0.10	Syenogranite
13	KST23-S4-191m	Alf: 12.00, Pl: 26.30, Qz: 39.20, Mos: 5.00, Bio: 8.00, Chl: 2.00, Kao: 2.50, Opa: 4.00, Amp: 1.00,	Granodiorite
14	KSC1-45m	Alf: 23.00, Pl: 20.30, Qz: 37.41, Mos: 3.00, Bio: 11.80, Chl: 2.5, Kao: 2.00, Opa: - , Amp: 0.00	Monzogranite
15	KST23-S6-206m	Alf: 50.60, Pl: 28.40, Qz: 8.00, Mos: 1.00, Bio: 10.00, Chl: -, Opa: 2.00, Amp: 0.00	Quartz monzonite

Qz: Quartz; Pl: Plagioclase; Alf: Alkali feldspar; Mos: Muscovite; Bio: Biotite; Amp: Amphibole; Chl: Chlorite; Kao: Kaolinite, Opa: Opaque minerals.



Figure 3. Cerchar abrasiveness testing device



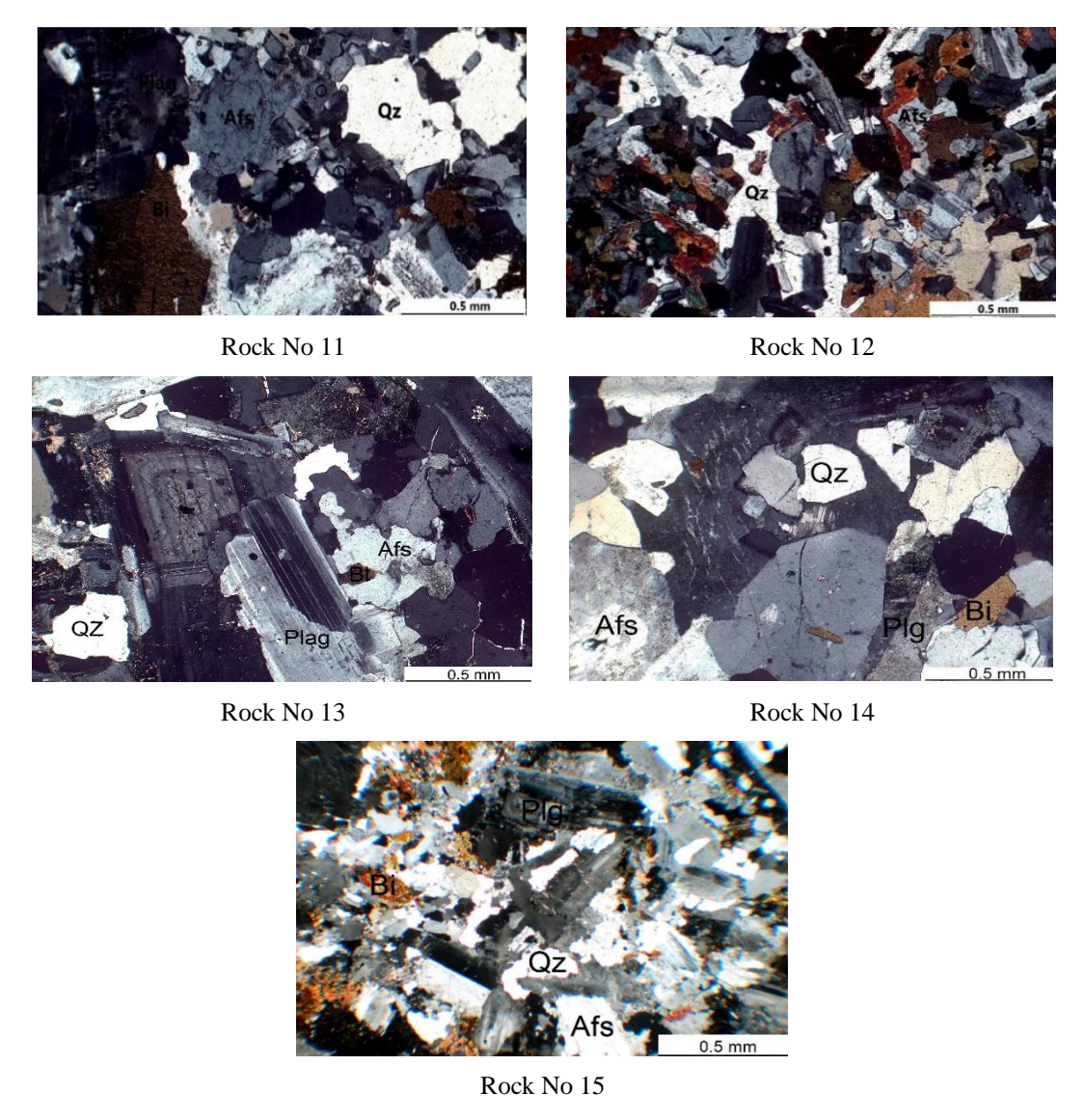


Figure 4. Thin sections are studied for petrographic analysis

Additionally, the thin sections were examined for the presence of opaque minerals, chlorite, amphibole, and muscovite, which are considered heavy and accessory minerals in the context of this study. The identification and characterization of these minerals provide valuable insights into the petrographic composition of the rocks.

Mineral contents have been quantified by calculating grains number from the thin section with the polarizing microscope. This method has the following steps: (1) taking images by digital microscopy, (2) image preparation, (3) extracting petrographic characteristics, and (4) performing regression analysis for precise investigation of petrographic and textural characteristics. Then, microscopic pictures of thin sections were considered by using Jmicro vision software v.1.27. The method of calculating the texture coefficient (TC) by JMicroVision V.1.27 software is shown in Figure 5. This software is open-source image processing and can quantifies (manually and automatically components) the common image processing operations.

One routine method to measure rock texture is using a texture coefficient (TC) technique, recommended by Howarth & Rowlands (1987). A number of scholars have applied TC to predict the geotechnical characteristics of rocks (e.g., Howarth & Rowlands, 1987; Ersoy & Waller, 1995; Singh & Verma, 2012; Ozturk & Nasuf, 2013; Ozturk et al., 2014; Tumac et al., 2017; Rostami et al., 2020; Karrari et al., 2023). The textural coefficient is determined by Eq. (1):

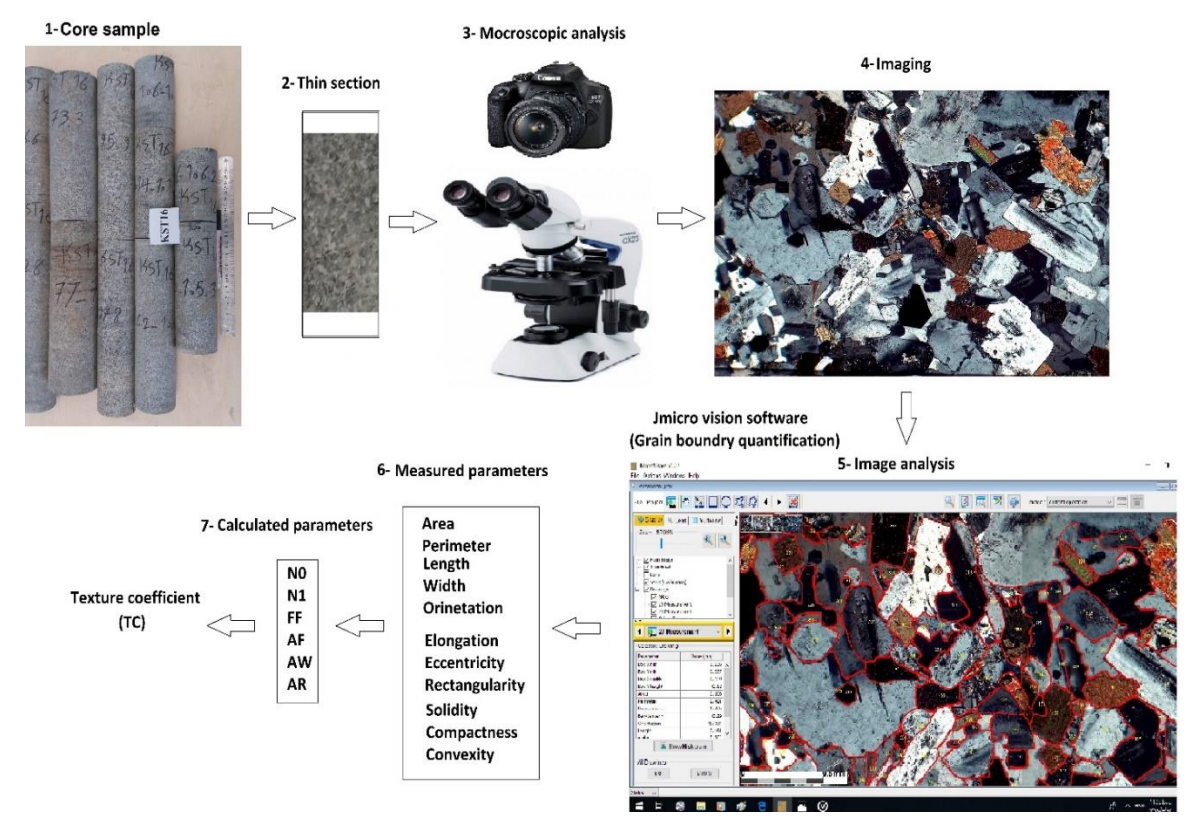


Figure 5. The method of calculating the texture coefficient (TC) by JMicroVision V.1.27 software

$$TC = AW \times \left[\left(\frac{N0}{N1 + N0} \right) \times \left(\frac{1}{FF0} \right) + \left(\frac{N1}{N1 + N0} \right) \times (AF1) \times (AR1) \right]$$
 Where.

TC: Textural coefficient

AW: Grain packing density (Area weighting)

N₀: The number of grains with an aspect ratio is less than a pre-set discrimination level of 2.

N₁: The number of grains with an aspect ratio is greater than a pre-set discrimination level of 2.

FF₀: Mathematics average of discriminated Form-Factors of all N₀ grains

AR₁: Mathematics average of discriminated aspect ratios of N₁ grains

AF₁: Angle Factor determining all N₁ grains orientation

In this study, microscopic images of the thin sections were analyzed using Jmicro Vision software version 1.27. The software facilitated the examination and analysis of the grain boundaries of the various rock components. To ensure accurate results, the software utilized a background registration procedure. Once the grain boundaries were calibrated and digitized, several parameters were automatically computed, including the minimum Feret's diameter, area, perimeter, maximum Feret's diameter, and the orientation of the individual grains. Feret's diameter is defined as being the perpendicular distance between two parallel, outer tangents to an object. These parameters provide quantitative measurements and insights into the size, shape, and spatial arrangement of the grains within the thin sections, enhancing the understanding of the rock's textural characteristics. In the end step, TC was determined by using Eq. (1). At least 250 grains are considered in each thin section to calculate the TC.

Acidic igneous rocks normally have four main minerals, including plagioclase, quartz, K-feldspar, and biotite, and accessory minerals (muscovite, Opaque) (Streckeisen, 1976). Various minerals usually have different grain sizes, which can be calculated with a heterogeneity index (H). The average grain size R_a is obtained as (Eq. (2)). The influence of material heterogeneity index is calculated as (Eq. 3) (Peng et al., 2017).

$$R_a = \sum_{i=1}^{m} (wi * ri)$$
 (2)

$$H = \sqrt{\sum_{i=1}^{m} (\frac{ri}{Ra} - 1)^2}$$
 (3)

Where r_i, W_i, m are the mean grain size of various minerals (mm), volume percentage, and the number of different major and minor minerals, respectively.

Grain size homogeneity Index (GI) is defined as a fabric factor, which explains the distribution of grain size in the rock (Eq. 4) (Karrari et al., 2023).

$$GI = \frac{Ag \, avg}{\sqrt{\sum (Agi - Ag \, avg)^2}}$$
 (4)

Where Ag_i is the individual grain area and Ag_{avg} is the average area of the grains.

Saturation Index (SI) is defined as the ratio of quartz percentage (Qtz) to the sum of feldspars (Alf + Pl) and quartz percentage (Eq. 5) (Karrari et al., 2023).

$$SI = \frac{Qtz\%}{(Alf+Pl+Qtz)\%}$$
 (5)

Feldspathic Index (FI) is defined as the percentage ratio of alkali-feldspars (Alf) to the sum of alkali-feldspars and plagioclase (Pl) percentage (Eq. 6) (Karrari et al., 2023).

$$FI = \frac{Alf\%}{(Pl + Alf)\%}$$
 (6)

Colouration Index (CI) is denoted as the sum volume of the light minerals (alkali-feldspars, plagioclase, and quartz) minus colored and dark minerals (muscovite, chlorite, amphibole, biotite, and opaque minerals) percentages in rock (Eq. 7) (Karrari et al., 2023).

$$CI = 100 - (Alf + Pl + Qtz) \%$$
 (7)

ABI (Abrasivity Index) is applied for estimating rock abrasiveness. ABI defined as multiple of two factors of Vickers hardness number of rock (VHNR) and UCS (Eq. 8) (Hassanpour et al., 2014; Hassanpour et al., 2019).

$$ABI = VHNR \times (UCS/100) \tag{8}$$

VHNR and UCS are the weighted mean of Vickers hardness number of particular minerals and uniaxial compressive strength based on MPa unit, respectively.

Rock Abrasivity Index (RAI) is included two factors: equivalent quartz content (EQC) and UCS (Eq. 9) (Plinninger, 2002).

$$RAI = UCS \times EQC = \sum_{i=1}^{n} UCS. mi. Ri$$
(9)

Where EQC, m_i, Ri, n, and UCS are the equivalent quartz content, the percentage of minerals, Rosiwal hardness that is estimated by using Rosiwal hardness of quartz, the total of major and minor minerals in a sample, uniaxial compressive strength, respectively. The Rosiwal hardness of each mineral is divided by the Rosiwal hardness of quartz, which quartz hardness is considered 100 percentage, and total other minerals' hardness will be compared to quartz. The Rosiwal hardness of the mineral will be modified for the ratio of each mineral in the rock sample, and the EQC of the rock will be calculated. In this study, Rosiwal hardness was determined according to Mohs hardness of the constituent minerals by using equation 10 (Ghasemi, 2010):

Rosiwal hardness =
$$\exp((Mohs hardness-2.12)/1.05)$$
 (10)

Schimazek's Sch value was specified through Schimazek & Knatz (1970) presented on Schimazek's pin-on-disc test mentioned by Verhoef (1997) (Eq. 11).

$$Sch = \frac{EQC* \phi* BTS}{100}$$
 (11)

Where, EQC is the equivalent quartz content (percentage), BTS is Brazilian tensile strength (MPa), and ϕ is the mean grain size of minerals (mm).

Results

Tables 4 and 5 present the results of petrographic and engineering features of 15 samples of acidic igneous rock. Textural parameters including the TC vary between 0.9 to 2.28, the H and

GI values range between 0.82 to 2.79, and 0.01 to 0.06, respectively. According to Ozturk & Nasuf classification (2013), TC values are high to very high.

Mineralogical indices, including the SI, FI, and CI values, ranges from 0.07 to 0.50, 0.32 to 0.90, and 6.70 to 40.04, respectively. According to Streckeisen classification (1976), SI values are quartzite to Feldspars rocks, FI values are Plagioclase to almost Alkali-feldspars, and CI values are Leucocratic and Hololeucocratic. These indices showed that these igneous rocks are categorized as felsic rocks.

Physical characteristics including porosity and dry unit weight values are from 0.47 % to 1.37 % and 26.00 kN/m³ to 28.06 kN/m³, respectively. Based on the Anon classification (1977), dry unit weight values vary from high to very high, and the porosity values vary from low to very low. Physical characteristics such as dry unit weight and porosity showed that these parameters depend on grain constituents, grain mineralogical, and rock texture (Roy, 2017). For example, the highest porosity is for rock number 4 that has the lowest TC, H, GI, SI, CI, CAI, ABI, and RAI.

The UCS test yielded results ranging from 40.56 MPa to 155.30 MPa, representing the compressive strength of the rock samples. On the other hand, the BTS test provided results ranging from 8.00 MPa to 18.81 MPa, indicating the tensile strength of the rock samples. I_{S50} test results are in the range of 5.3 to 9.27 MPa, and Et values are from 23.43 MPa to 85.80 MPa. Based on the ISRM classification (2007), the UCS values vary from low to high. According to the Bieniawski classification (1975), the I_{S50} values vary from high to very high. Mechanical properties showed that these igneous rocks have high compressive and tensile strength.

The Sch values range from 1.21 to 5.06, representing the Schimazek abrasivity index. The CAI values range from 1.17 to 4.48, indicating the Cerchar Abrasivity Index. The ABI values range from 279.05 to 1334.5, representing the Abrasivity Index of Bituminous Coal. Lastly, the RAI values range from 4.35 to 95.79, indicating the Rock Abrasivity Index. According to the Plinninger classification (2010), the RAI values vary from non-abrasive to very abrasive rocks. Based on the Alber et al. (2014) classification, the CAI values are low to very high. Abrasivity indices showed that these igneous rocks have low to very high abrasiveness.

In this study, experimental investigations including textural parameters, mineralogical indices, physical properties, and mechanical properties showed that most samples have high TC, H, SI, CAI, ABI, and RAI values. To evaluate the relationships between CAI with petrographical, textural, and mechanical rock characteristics, statistical analyses were used.

Table 4. Petrographic features of rock samples

		Mineralogical indices									
Rock No	Area (mm²)	Perimeter (mm)	Min of Feret's (mm)	Max of Feret's (mm)	Size (mm)	TC	Н	GI	SI	FI	CI
1	0.10	1.39	0.25	0.44	0.28	1.76	2.37	0.05	0.21	0.60	10.86
2	0.07	0.58	0.12	0.29	0.13	1.72	1.88	0.02	0.22	0.69	40.04
3	0.30	2.41	0.53	0.77	0.56	1.51	1.70	0.04	0.18	0.85	12.16
4	0.37	2.97	0.80	0.95	0.88	0.99	0.85	0.02	0.07	0.90	5.30
5	0.04	0.99	0.18	0.29	0.15	2.03	2.79	0.06	0.19	0.60	29.96
6	0.04	0.91	0.18	0.30	0.20	1.91	1.90	0.03	0.16	0.61	22.54
7	0.20	1.10	0.40	0.69	0.25	1.40	1.36	0.03	0.14	0.82	16.11
8	0.08	1.01	0.29	0.40	0.22	1.54	1.44	0.03	0.20	0.81	21.04
9	0.18	1.82	0.37	0.59	0.30	1.82	2.37	0.04	0.34	0.70	15.93
10	0.20	2.01	0.32	0.55	0.42	1.78	1.99	0.06	0.31	0.60	26.63
11	0.07	0.88	0.17	0.28	0.29	1.71	1.69	0.01	0.27	0.78	11.98
12	0.06	0.96	0.19	0.31	0.20	1.80	1.66	0.02	0.23	0.76	28.98
13	0.15	1.61	0.31	0.50	0.40	2.28	2.25	0.03	0.50	0.32	6.70
14	0.10	1.40	0.20	0.60	0.40	2.15	2.30	0.05	0.43	0.60	6.70
15	0.35	2.90	0.75	0.90	0.83	0.90	0.82	0.02	0.09	0.88	12.60

Table 5. Engineering features of rock samples

Physi	cal characte	ristics	M	echanical c	haracteris	tics	•	Abrasivity indices			
Rock No	Dry unit weight (KN/m ³)	Porosity (%)	UCS (MPa)	BTS (MPa)	I _{S50} (MPa)	Et (MPa)	Sch	CAI (mm/10)	ABI	RAI	
1	25.89	1.23	115.80	16.45	7.93	44.82	3.06	3.10	860.21	62.13	
2	27.86	0.47	127.35	18.18	8.92	59.03	3.08	2.59	655.24	42.07	
3	26.09	0.76	118.98	16.52	5.76	49.22	1.33	2.76	807.04	56.19	
4	26.09	1.37	40.56	8.31	5.83	23.43	5.06	1.17	279.05	18.89	
5	26.68	0.64	128.66	12.22	6.84	30.71	3.39	3.19	773.60	54.08	
6	26.88	0.60	149.13	18.35	8.85	39.65	1.21	2.86	965.40	66.64	
7	28.05	1.026	71.78	7.33	5.50	76.41	1.96	2.21	443.82	30.33	
8	27.86	1.256	59.49	10.76	5.04	45.35	1.68	2.37	365.53	35.11	
9	27.27	0.615	97.24	12.50	9.27	27.34	1.62	3.48	706.24	53.52	
10	26.29	0.749	107.06	12.81	6.57	40.60	3.30	3.06	745.78	50.95	
11	26.38	0.608	115.86	14.03	6.57	47.65	2.84	2.88	863.56	64.83	
12	26.88	0.346	125.51	14.43	7.92	44.94	1.76	2.27	942.04	53.25	
13	26.48	0.800	155.30	18.81	8.92	85.80	4.90	4.48	1334.5	95.79	
14	25.99	0.850	120.50	15.75	5.30	45.65	3.03	4.00	1012.4	60.59	
15	26.29	1.300	45.34	8.00	5.50	24.50	5.00	1.30	340.45	4.35	

Statistical analysis

In this research, statistical analyses were conducted to explore the relationships between the CAI, petrographic and textural features, and engineering properties of the acidic igneous rocks. Various statistical methods, including linear and nonlinear regression analysis and bivariate correlation, were employed to assess the potential correlations between these variables. The statistical results obtained from these analyses were thoroughly investigated and evaluated. The goal was to identify and select the most suitable models that effectively capture the relationships between CAI, petrographic and textural features, and engineering properties. This approach allowed for a comprehensive understanding of the factors influencing the rock's abrasiveness and provided valuable insights for engineering and construction applications.

Pearson's correlation coefficient

Pearson's correlation coefficient (R) was applied to study the efficiency and significant correlation between CAI with petrographical, textural, and engineering features (Eq. 12). $R_{xy} = COV x, y / SDx. SDy$ (12)

Where the Pearson's correlation ($R_{x,y}$) between the covariance values ($COV_{x,y}$) divided by their standard deviations (SD_x and SD_y) is determined, in Table 6, Pearson's correlation coefficients, the CAI, petrographic features, and engineering characteristics are revealed. Significance of regression was calculated using hypothesis test (P-value) proposed by Johnson (1998). The P-value less than 0.05 shows that it is statistically significant at a 95 % confidence level. Many researchers used this method to evaluate their results (e.g., Khaleghi Esfahani et al., 2019; Torrijo Garzón-Roca, 2020; Karrari et al., 2023). There is a significant relationship between CAI and engineering features, including P values of TC, H, SI, FI, BTS, UCS, ABI, and RAI are lower than 0.05 (Table 6). The best correlation is between CAI and TC (R = 0.929). It shows that rock texture is an impressive factor for rock abrasivity in felsic igneous rocks. Also, CAI and SI have a high correlation (R = 0.895), display that the mineralogy (quartz content) is an effective factor to estimate rock abrasivity in felsic igneous rocks. Relationships between CAI with textural indices (TC, H) and petrographical indices (SI, FI) indicate rock texture and mineralogical parameters are effective parameters for estimating CAI. Aligholi et al. (2018) reported fabric and mineralogical properties are significantly effective for predicting engineering features.

	Table of Tearson's conference and significant level											
Properties correlation		Textural indices		alogical ices	Physical characteris tics	Mechanical characteristics			Abra	sivity in	dices	
Pearson's correlation	TC	Н	SI	FI	P (%)	UCS (MPa)	BTS (MPa)	I _{S50} (MPa)	Sch	ABI	RAI	
CAI(R)	0.929	0.850	0.895	-0.845	- 0.435	0.771	0.681	0.420	- 0.445	0.863	0.888	
P value	0.000	0.000	0.006	0.000	0.053	0.001	0.005	0.119	0.116	0.000	0.000	

Table 6. Pearson's correlation coefficients and significant level

R: P-value: Significance level (0.05), Pearson's correlation coefficients, CAI: Cerchar abrasion index, TC: texture coefficient, H: heterogeneity index, SI: Saturation Index, FI: Feldspathic Index, P: porosity, UCS: uniaxial compressive strength, BTS: Brazilian tensile strength, I_{S50}: point load index, Sch: Schimazek F value, ABI: abrasion index, RAI: rock abrasiveness index. *significant at 95% confidence level

Increasing the CAI is linked to several changes in the petrographical and engineering characteristics of acidic igneous rocks. Petrographical features such as Texture Coefficient (TC), Heterogeneity (H), and Saturation Index (SI) show an increase as CAI values rise. Similarly, engineering properties like Uniaxial Compressive Strength (UCS), Abrasivity Index (ABI), and Rock Abrasivity Index (RAI) also increase with higher CAI values. However, there is a negative correlation (-0.845) between CAI and the content of alkali-feldspars (FI), indicating a decrease in FI as CAI increases.

The correlation analysis in this study revealed that the weakest correlation (R = 0.420) was observed between the $I_{\rm S50}$ and CAI. The significance level (p-value) for this correlation was found to be less than 0.05, indicating poor significance. This weaker correlation might be attributed to the mechanism of the point load test. Additionally, an inverse correlation (R=0.435) was identified between porosity and CAI. This indicates that as the CAI value increases, the porosity tends to decrease. Also, Abu Bakar et al. (2016) and Rostami et al. (2020) described an inverse correlation between CAI and porosity. The inverse relationship between porosity and CAI may be due to low strength, and hardness of rock samples.

The inverse correlation between the Feldspathic Index (FI) and Cerchar Abrasivity Index (CAI) can be attributed to the lower hardness of feldspathic grains compared to quartz. With a hardness of 6-6.5 on Moh's scale, feldspar grains are softer than quartz (hardness of 7). On the other hand, the CAI shows a positive relationship with the Abrasivity Index (ABI), Rock Abrasivity Index (RAI), grain hardness, and rock strength. As these factors increase, so does the CAI, indicating a higher level of abrasiveness. Thus, grain hardness and rock strength play a significant role in determining the CAI and the overall abrasiveness of rocks. Majeed & Abu Bakar (2015) reported a logarithmic relationship between RAI and CAI. Their research showed that rock strength and hardness increased with increasing CAI.

Simple regression analysis

In the following, relations between CAI and engineering features have been examined. While the relation between the dependent and independent variables is not essentially linear, the non-linear (curve) estimation must be applied (Norusis, 2002). In linear and non-linear regression analysis, the good curve estimations such as 6 models: linear $(y = a_1. CAI + c)$, inverse $(y = (a_1 CAI) + c)$, logarithmic $(y = (a_1. Ln (CAI) + c)$, quadratic $(y = (a_1. CAI) + (a_2. CAI^2) + c)$, exponential $(y = (exp (a_1. CAI)). c)$, and power $(y = CAI^{a_1. c})$. Y is the dependent variable, c is a constant value, a_1 and a_2 are regression coefficients.

The efficiency of the statistical analysis were evaluated by normal statistical techniques, such as the coefficient of determination (R^2), adjusted R^2 (Adj R^2), analysis of variance (ANOVA), and standard error (Std. Er). The R^2 and Adj R^2 applied to assess regression models' validity. Higher R^2 (R^2 =1) values show more accurate relationships in linear regression. While R^2 is a

well statistical factor, only a greater value of R² is not suitable for comparing between 2 regression models (Omar, 2016). Consequently, two error methods were used for evaluating relationships. The Mean absolute percentage error (MAPE) and root means square error (RMSE) for assessing each model is determined by Eqs. 13 and 14, respectively. The MAPE percentage for the assessment models shows in Table 7.

MAPE =
$$\frac{\sum_{i=1}^{n} \left| \frac{Y_i - X_i}{Y_t} \right|}{n} \times 100$$
 (13)
RMSE = $\sqrt{\frac{1}{n}} \sum_{i=1}^{n} (Y_i - X_i)^2$

RMSE =
$$\sqrt{\frac{1}{n}} \sum_{i=1}^{n} (Yi - Xi)^2$$
 (14)

Where Y_i is the measured value, X_i is the predicted value, and n is a number of samples. If $R^2 = 1$, MAPE < 10%, and RMSE = 0, the suggested model would be excellent.

Simple regression analyses were conducted between petrographic, textural, mechanical characteristics, and CAI for determining these properties. Table 8 shows the best models for engineering features. The best regression analysis between CAI and examined engineering features (TC, H, SI, UCS, ABI, and RAI) was the power model (Table 8).

Textural properties (TC and H) displayed that a good correlation between CAI, TC, and H (Table 8). The correlation between CAI, and petrographical, mechanical, and abrasivity characteristics is indicated in Figure 6. Statistical analyses show that CAI has a better correlation with TC ($R^2 = 0.898$, RMSE = 0.562, MAPE = 12.697) than H ($R^2 = 0.862$, RMSE = 0.485, MAPE = 10.677). As previously, mentioned, TC encompasses grain size, grain direction, and grain packing. H include different grain sizes minerals (grain size and volume fraction). So, TC encompasses more parameters of rock texture than H. Neither TC nor H do not represent the composition and mineralogy of grains.

Petrographical indices (SI, FI) showed the percentage and type of minerals. The good correlation between petrographical indices is SI ($R^2 = 0.837$, RMSE = 0.364, MAPE = 12.017). The saturation index is better than the feldspathic index for comparing CAI because it includes quartz content, and feldspathic minerals have low abrasiveness specific. Undul & Er (2017) indicated increasing feldspar, plagioclase, and opaque minerals due to a reduction in CAI values. Er & Tugrul (2016) mentioned that the quartz content of the granitic rocks increased CAI. Aligholi et al. (2018) showed a direct relation between CAI, SI, and FI with correlation coefficients (R = 0.80 and R = 0.69), respectively.

Table 7. Evaluation of models MAPE percentage (McKenzie 2011; Leys et al. 2013)

MAPE (%)	Evaluation
MAPE < 10%	excellent
10% < MAPE < 20%	good
20% < MAPE < 50%	reasonable
MAPE > 50%	poor

Table 8. The best simple regression analyses between CAI and engineering features

Number equation	Equation	R	\mathbb{R}^2	Adjusted R ²	Standar d error	F	Sig	RMSE	MAPE
15	$CAI = 1.363 \text{ TC}^{1.328}$	0.948	0.898	0.890	0.120	114.292	0.000	0.562	12.697
16	$CAI = 1.562 \text{ H}^{0.948}$	0.929	0.862	0.852	0.140	81.376	0.000	0.485	10.677
17	$CAI = 7.020 SI^{0.627}$	0.915	0.837	0.824	0.152	66.554	0.000	0.364	12.017
18	CAI = 4.768 - 0.007 FI - 3.867 FI ²	0.874	0.763	0.724	0.459	19.345	0.000	0.433	15.335
19	$CAI = 0.089 \ UCS^{0.738}$	0.851	0.725	0.703	0.198	34.193	0.000	0.645	16.927
20	$CAI = 0.291 BTS^{0.857}$	0.730	0.533	0.497	0.257	14.830	0.002	0.621	21.959
21	$CAI = 0.028 ABI^{-0.700}$	0.868	0.753	0.734	0.187	39.665	0.000	0.518	15.028
22	$CAI = 0.547 \text{ RAI}^{-0.419}$	0.850	0.722	0.700	0.199	33.732	0.000	0.507	16.387

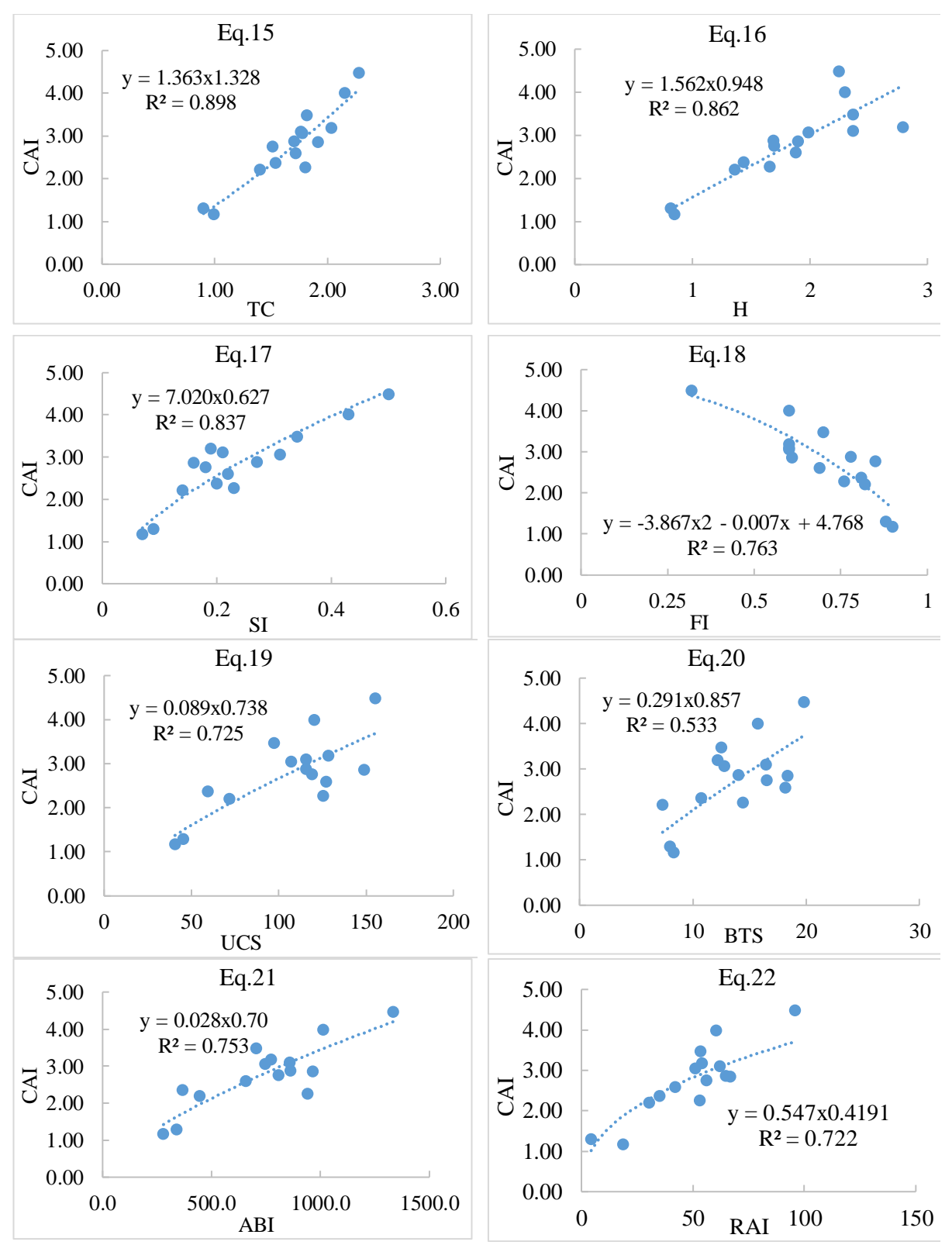


Figure 6. The correlation between CAI, petrographical, mechanical, and abrasivity characteristics

Mechanical characteristics revealed that a reasonable correlation exists between CAI and UCS with a 0.725 coefficient of determination and 0.645 and 16.927 RMSE and MAPE (Table 8, Eq. 19). Because rock compressive strength is resistance to indentation pin to rock performed test. Similar relations between CAI and UCS were presented in other studies (Ko et al., 2016; Rostami et al., 2020). Abrasiveness characteristics showed that the good correlations between CAI, ABI, and RAI

with R²= 0.753, RMSE = 0.518, MAPE = 15.028 and R²= 0.722, RMSE = 0.507, MAPE = 16.387 were presented in Table 8 (Eq. 21 and 22), respectively. ABI has two good statistical parameters and has a lower MAPE and higher R² in comparison with RAI. Considering, ABI composing of Vickers hardness was showed more effective than RAI that composing of equivalent quartz content. Vickers hardness has the cubic indentation to rock penetration. However, EQC has been calculated from Rosiwal hardness that this quantified by Moh's hardness scale. Moh's hardness scale indicated relative hardness and did not determine a precise hardness value. Majeed & Abu Bakar (2015) reported a logarithmic relationship between RAI and CAI with coefficient determination from 0.43 to 0.53.

The initial analysis indicated that mechanical characteristics and abrasivity indices have the potential to be utilized for estimating the Cerchar Abrasivity Index (CAI). To improve the accuracy of the predictions, further analysis was conducted using multiple linear and non-linear regression techniques, aiming to enhance the R^2 value.

Multiple Linear Regression (MLR) and Non-Linear Regression (MNLR)

The multiple linear and non-linear regression analyses were applied to acquire the best-fit empirical relations. In this research, statistical analyses were conducted by two and three independent variables with the status that one of the independent variables was a CAI. Consequently, Eqs. 23 and 24 are presented to estimate CAI based on geomechanical characteristics.

$$CAI = \alpha_0 + \alpha_1. X_1 + ... + a^n. X^n$$
 (23)

$$CAI = \alpha_0 + \alpha_1. X_1^{\alpha_2} + ... + \alpha_n. X_n^{\alpha_n}$$
(24)

Where CAI, X_1 , and X_n are the geomechanical characteristics, α_0 is a constant, α_1 , α_2 , and α_1 are the regression coefficients of X_1 , and X_n respectively. The power multiple non-linear regression analyses were applied to determine the empirical relations. Since this equation in preliminary examination indicated a good R^2 , RMSE, and MAPE. Unique evaluation multiple linear equations were presented in Table 9 (Eqs. 25 to 36). In this table, the correlation coefficient (R^2), adjusted correlation (R^2), standard error, the significance values, F statistics, MAPE, and RMSE values were applied to assess and quantify the presented models' accuracy. In addition, for easy understanding, the MLR models are shown the number equations (Eqs. 25 to 36) against R^2 , RMSE, and MAPE in Figure 7.

Table 9. Results of multiple linear regression analysis between TC, H, ABI, RAI, SI, FI and CAI

Number equation	Equation	R	\mathbb{R}^2	Adjusted R ²	Standard error	F	sig	RMSE	MAPE
25	CAI = - 0.250 + 3.108 SI + 1.360 TC	0.963	0.927	0.915	0.254	76.630	0.000	0.320	8.190
26	CAI = 1.032 - 1.451 FI + 1.638 TC	0.939	0.881	0.861	0.325	44.335	0.000	0.454	11.177
27	CAI = - 0.187 + 1.225 TC + 0.001 UCS + 3.230 SI	0.963	0.928	0.908	0.264	47.222	0.000	0.321	8.147
28	CAI = 0.946 + 1.953 TC - 0.004 UCS - 1.482 FI	0.942	0.887	0.857	0.330	28.856	0.000	0.454	11.485
29	CAI = 0.376 + 4.405 SI + 0.746 H	0.969	0.940	0.930	0.231	93.337	0.000	0.219	7.045
30	CAI = 3.528 - 2.952 FI + 0.723 H	0.915	0.836	0.809	0.381	30.658	0.000	0.363	12.290
31	CAI = 3.195 + 0.654 H + 0.003 UCS - 2.687 FI	0.917	0.840	0.797	0.393	19.292	0.000	0.367	12.663
32	CAI = 0.302 + 0.588 H + 0.004 UCS + 4.187 SI	0.975	0.950	0.937	0.219	69.913	0.000	0.213	6.386
33	CAI = -0.549 + 0.001 ABI + 1.655 TC	0.937	0.879	0.859	0.328	43.526	0.000	0.487	11.475
34	CAI = 0.318 + 0.001 ABI + 0.614 H + 3.497 SI	0.981	0.962	0.952	0.191	93.721	0.000	0.282	9.556
35	CAI = -0.405 + 0.012 RAI + 1.545 TC	0.938	0.881	0.861	0.325	44.268	0.000	0.498	11.923
36	CAI = 0.399 + 0.011 RAI + 0.562 H + 3.442 SI	0.979	0.958	0.947	0.200	84.476	0.000	0.195	6.094

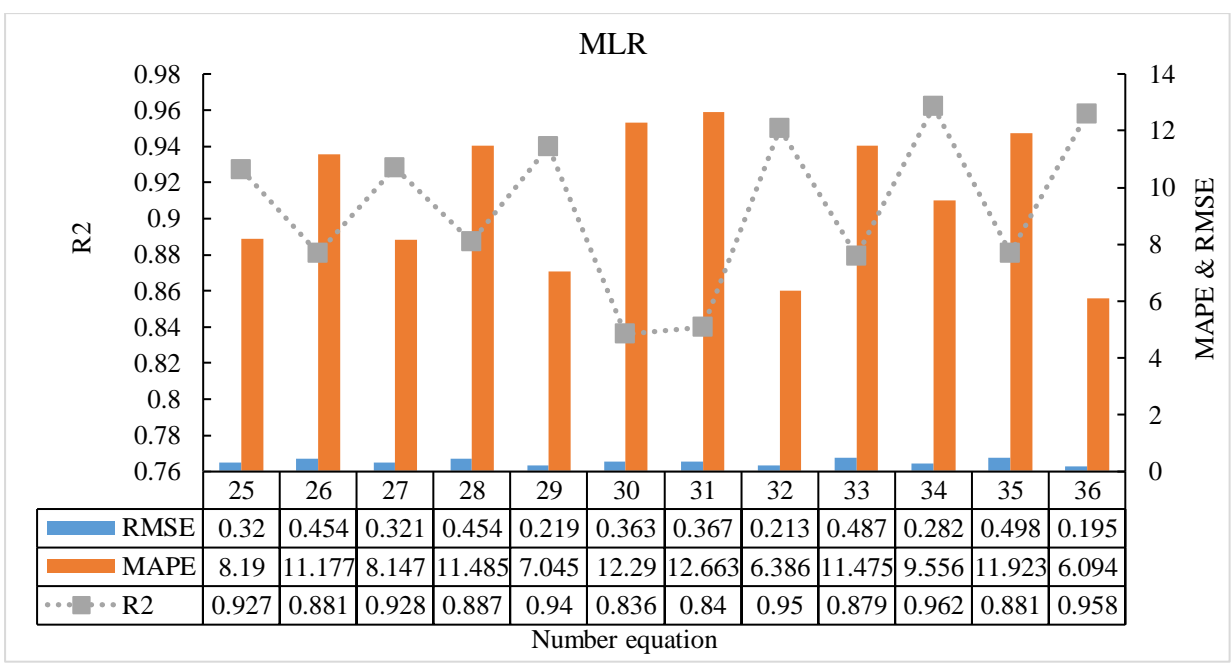


Figure 7. The number equations (Eqs. 25 to 36) against R², RMSE, and MAPE in MLR models

The MLR and MNLR models were used at a significance level of 0.95. The verification of presented equations between TC, H, SI, FI, UCS, ABI, and RAI, is used to estimate CAI. In addition, the variance analysis technique is applied for investigating the significance of regression in multiple linear and non-linear regressions. The results displayed that amid totally the multiple linear regression analyzed parameters H, ABI, and SI showed the best fit with CAI ($R^2 = 0.962$, RMSE = 0.282, MAPE = 9.556) (Eq. 34, Table 8). This equation has an excellent relationship because it has the highest R² and lowest RMSE and MAPE (Eq. 34). Results showed that the good multiple linear regression analyzed parameters RAI, H, and SI showed the best fit with CAI $(R^2 = 0.958, RMSE = 0.195, MAPE = 6.094)$ (Eq. 36, Table 8). These equations (Eqs. 34 and 36) revealed the influence of mineralogical properties (SI), textural properties (H), hardness, and rock strength (ABI) on CAI. The comparison between two equations, 29 and 30, revealed a significant relation. The H has better relation with SI rather than FI for estimating CAI, respectively (R^2 = 0.940, RMSE = 0.219, MAPE = 7.045 and $R^2 = 0.836$, RMSE = 0.363, MAPE = 12.290). Also, comparison between two equations 25 and 26 indicated that the TC have better relation with SI $(R^2 = 0.927, RMSE = 0.320, MAPE = 8.190)$ rather than FI $(R^2 = 0.881, RMSE = 0.454, MAPE$ = 11.177) for estimating CAI. The reason may be related to the content of quartz with different sizes. Because by increasing quartz, heterogeneity, and CAI increases. Also, the relation between TC and FI may be connected to alkali feldspar subhedral grain shape, and TC is affected from N_0 , N_1 , and FF_0 (Eq. 1). The comparison between two equations 25 and 29 showed that the H has better relation with SI rather than TC with SI for estimating CAI, respectively ($R^2 = 0.927$, RMSE = 0.320, MAPE = 8.190 and $R^2 = 0.940$, RMSE = 0.219, MAPE = 7.045). The different minerals sizes (H) are more effective than TC on CAI. When pin is scratched on rock samples, various minerals size and quartz content may cause increasing CAI value. The comparison of three equations 32, 34, and 36 indicated that the rock strength is more effective than hardness. Also, ABI is more effective than RAI.

Table 10 indicates the multiple non-linear regression relations (Eqs. 37 to 48). Additionally, for easy understanding, the MNLR models showed the number equations (Eqs. 37 to 48) against R^2 , RMSE, and MAPE in Figure 8. In this Table, the results of multiple nonlinear regression analyses between TC, H, ABI, RAI, SI, FI, and CAI are presented. Amid totally the multiple non-linear regression analyzed parameters, ABI, H, and SI displayed the best fit with CAI ($R^2 = 0.972$, RMSE = 0.148, MAPE = 5.039 (Table 10, Eq. 46). Results displayed that the good

multiple non-linear regression analyzed parameters UCS, H, and SI showed the best fit with CAI ($R^2 = 0.970$, RMSE = 0.151, MAPE = 5.068) (Table 10, Eq. 44). These relationships (Eqs. 46 and 44) have the highest R^2 and lowest RMSE and MAPE.

Analysis of the relationships revealed that the relationship between H and the independent variables (CAI, UCS, FI, SI) is better than TC. As previously mentioned, the H parameter is more efficient than TC. The assessment between two equations, 41 and 43, displayed that the R², RMSE, and MAPE are approximately similar. Equation 43 has 3 independent variables (UCS, H, and FI), but Equation 41 has 2 independent variables (H and FI). These relations revealed that the UCS does not have a significant influence on CAI. So, textural and mineralogical properties are more effective than rock strength.

Generally, these relationships are based on higher R² and lower RMSE and MAPE. They showed that nonlinear equations (Table 10) had relatively better results than linear equations (Table 9).

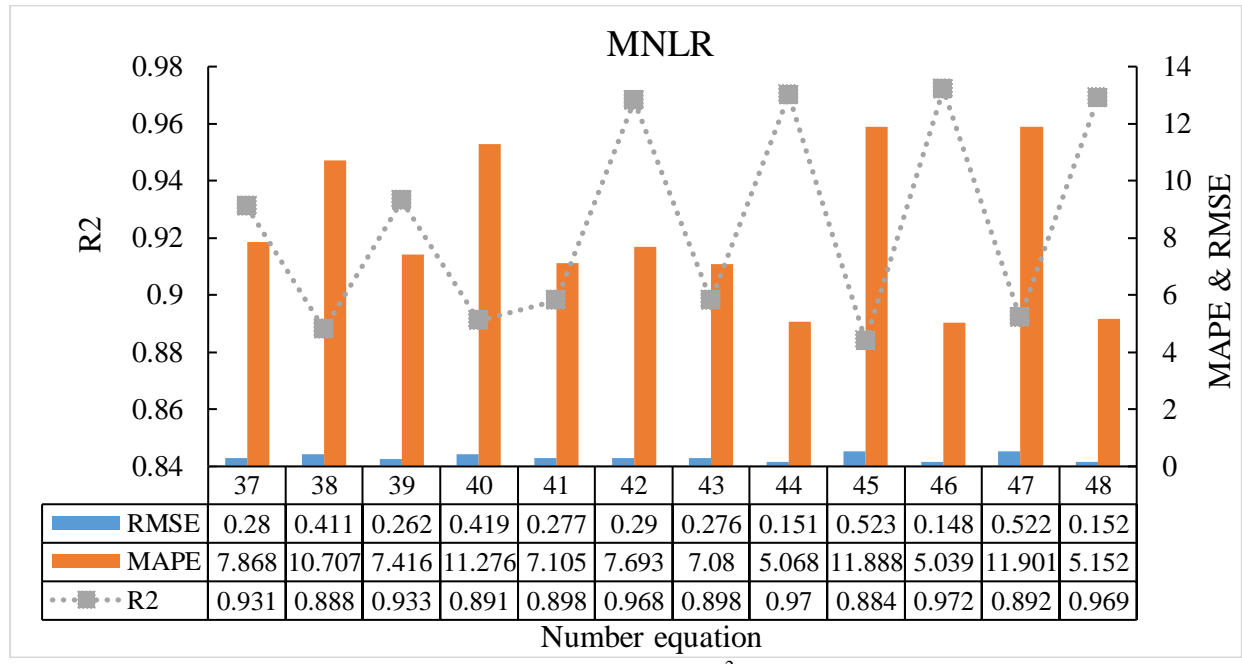


Figure 8. The number equations (Eqs. 37 to 48) against R², RMSE, and MAPE in MNLR models

Table 10. Results of multiple nonlinear regression analysis between TC, H, ABI, RAI, SI, FI and CAI

Number equation	Equation	R	\mathbb{R}^2	Adjusted R ²	Standard error	F	sig	RMSE	MAPE
37	CAI = $-8.758 + 10.136$ TC $^{0.2} + 5.898$ SI $^{2.177}$	0.964	0.931	0.923	0.274	128.554	0.000	0.280	7.868
38	CAI = $-4.363 + 5.438$ TC $^{0.4} + 0.262$ FI $^{-1.398}$	0.942	0.888	0.876	0.144	76.468	0.000	0.411	10.707
39	$CAI = -81.849 + 8.439$ $TC^{0.2} + 73.977 UCS$ $^{0.003} + 5.918 SI^{2.102}$	0.965	0.933	0.926	0.100	169.677	0.000	0.262	7.416
40	CAI = - 2.842 + 6.217 TC ^{0.4} - 1.559 UCS ^{0.1} + 0.259 FI ^{-1.391}	0.943	0.891	0.878	0.149	69.987	0.000	0.419	11.276
41	CAI = -16.418 + 18.016 $H^{0.1} + 0.015 FI^{-3.962}$	0.947	0.898	0.889	0.296	108.645	0.000	0.277	7.105
42	CAI = $-13.971 + 15.577$ H $^{0.1} + 14.209$ SI $^{3.171}$	0.983	0.968	0.964	0.076	303.767	0.000	0.290	7.693
43	CAI = - 16.415 + 18.120 H 0.1 - 0.072 UCS 0.1 + 0.015 FI -3.969	0.947	0.898	0.889	0.296	108.840	0.000	0.276	7.080

These equations showed that the model fits the data well and can estimate CAI, petrographical indices (SI and FI), and textural features (TC and H), abrasiveness properties (ABI and RAI) with acceptable accuracy.

Artificial Neural Network (ANN)

The artificial neural network (ANN) is a statically model based on the configuration and functions of biological neural networks. The ANN modeling instrument is applied for establishing relations between inputs and outputs non-linear and intricate (Mishra et al., 2015). The ANN model applied for this research is a multi-layer perceptron (MLP) (Fig. 9a, b). The configuration of ANN models contains 2 and 3 inputs, 5 and 7 neurons in the hidden layer, and one output (Fig. 9a, b). Hecht-Nielsen (1987) suggested the number of hidden layers for ANN model, applied in this study, is ≤ 2 (inputs) + 1. The ANN model was made through Matlab software version R2016a.

The artificial neural network (ANN) model used in this study was trained through repeated exposure to input and output data. The goal of the training process was to minimize the error between the model's output and the experimental output. To achieve this, the Levenberg-Marquardt algorithm, which is a second-order algorithm known for its efficiency in training medium-sized feedforward ANN models, was employed. This algorithm is a type of backpropagation neural network architecture that utilizes the gradient descent error optimization method (Ticknor, 2013).

In this research, the percentage for training and test ANN analysis is 85% and 15%, respectively. The input variables (TC, H, SI, FI, UCS, ABI, and RAI) were used to estimate CAI. The ANN models were offered in Table 11 (Models. 49 to 60). For easy understanding, the MNLR models showed the number equations (Eqs. 49 to 60) against R², RMSE, and MAPE in Figure 10. The best ANN model analysis was obtained between ABI, CAI, TC, and, SI (R² = 0.974, RMSE = 0.137, MAPE = 4.610) (Table 11; Model. 58). The good ANN model presented between CAI, and H, UCS, and SI (R² = 0.973, RMSE = 0.131, MAPE = 4.678) (Table 11; Model. 56). ANN results show high accuracy for estimating CAI. ANN model analyses have higher R, R², adjusted R², and F statistics in comparison with The MLR and MNLR analysis. Also, the results displayed a reduction in the RMSE and MAPE values between the ANN analyses in comparison with MLR and MNLR analyses. Overall, ANN outperformed the MLLR and MLR models.

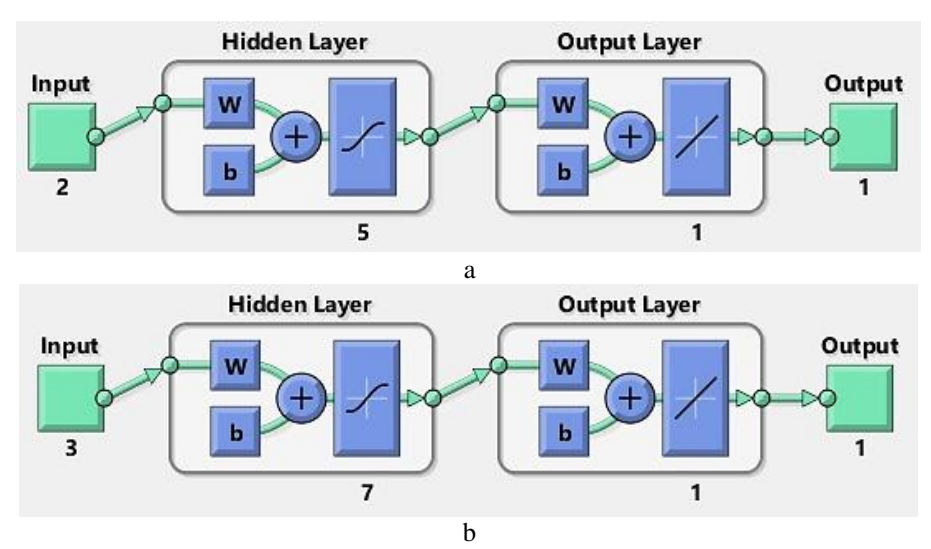


Figure 9. General scheme of ANN models structure. a) The architecture of model includes 2 inputs, 5 hidden layers, one input. b) The architecture of model includes 3 inputs, 7 hidden layers, and one output

	Tubic III	Ttoburto of Th	ii i diidi	<i>J</i> 515 C C 1	meen depe	macini ana i	macpe me	toric tar	140105	
Number model	Dependent variables	Independent variables	R	\mathbb{R}^2	Adjusted R ²	Standard error	F	sig	RMSE	MAPE
49	CAI	TC, SI	0.969	0.940	0.935	0.068	200.69	0.000	0.224	5.755
50	CAI	TC, FI	0.957	0.915	0.909	0.081	140.02	0.000	0.096	4.631
51	CAI	TC, UCS, SI	0.972	0.945	0.940	0.065	221.82	0.000	0.213	6.386
52	CAI	TC, UCS, FI	0.963	0.928	0.922	0.074	167.41	0.000	0.243	7.677
53	CAI	H, SI	0.985	0.970	0.968	0.048	423.50	0.000	0.156	4.578
54	CAI	H, FI	0.964	0.930	0.924	0.073	172.25	0.000	0.240	5.554
55	CAI	H, UCS, FI	0.954	0.910	0.903	0.083	131.37	0.000	0.272	7.545
56	CAI	H, UCS, SI	0.986	0.973	0.972	0.040	609.70	0.000	0.131	4.678
57	CAI	ABI, TC	0.953	0.908	0.901	0.084	128.26	0.000	0.275	8.527
58	CAI	ABI, SI, H	0.987	0.974	0.971	0.039	494.37	0.000	0.137	4.610
59	CAI	RAI, TC	0.957	0.915	0.909	0.081	140.53	0.000	0.264	6.481
60	CAI	RAI, SI, H	0.985	0.970	0.968	0.048	426.40	0.000	0.156	4.311

Table 11. Results of ANN analysis between dependent and independent variables

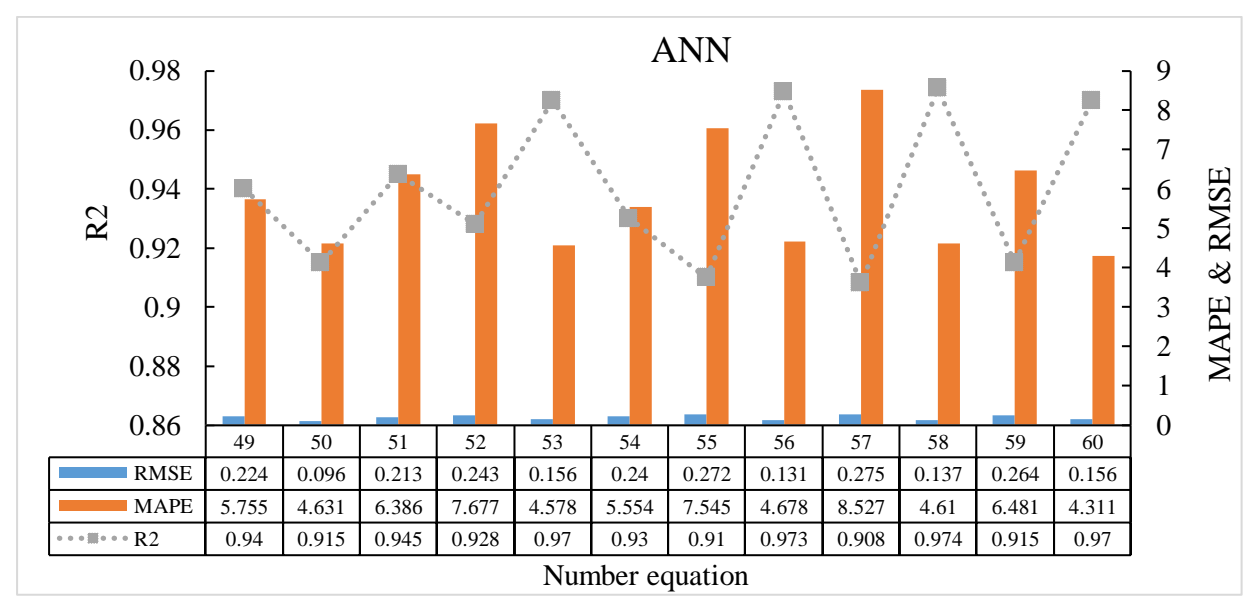


Figure 10. The number equations (Eqs. 37 to 48) against R², RMSE, and MAPE in MNLR models

Discussion

The results show that increasing the CAI is related to the petrographical and engineering characteristics of acidic igneous rocks. Petrographical features such as TC, H, and SI show an increase in CAI values. The CAI and SI have a high correlation coefficient (R = 0.895). Aligholi et al. (2018) described mineralogical and fabric properties are significantly effective for predicting engineering features. He showed a direct relation between CAI and SI with a correlation coefficient equal to 0.80. SI displays that the quartz content is an effective factor in estimating rock abrasivity in felsic igneous rocks. SI is better than FI for comparing CAI because it includes quartz content, and feldspathic minerals have low abrasiveness specific. Undul & Er (2017) showed increasing feldspar, plagioclase, and opaque minerals due to a decrease in CAI values. Er &Tugrul (2016) stated that the quartz content of the granitic rocks increased CAI.

Additionally, an inverse correlation was identified between CAI and porosity. This shows that as the CAI value increases, the porosity tends to decrease. Abu Bakar et al. (2016) and Rostami et al. (2020) defined an inverse correlation between CAI and porosity.

A reasonable correlation exists between CAI and UCS with a 0.725 coefficient of

determination.

Er &Tugrul (2016), Undul &Er (2017), Ko et al. (2016), and Rostami et al. (2020) showed that the CAI of magmatic rocks with UCS increased.

In multiple linear and non-linear regression and ANN analysis CAI, ABI, H, and SI revealed the highest correlation (Table 9, Eq.34; Table 10, Eq.46; Table 11, Eq.58). The results of the analysis indicate that SI, H, and ABI are suitable parameters for comparing the abrasiveness of acidic igneous rocks. These parameters include quartz content, rock texture, strength, and hardness which affect CAI. Aligholi et al. (2018) presented a multiple linear regression analysis between CAI and petrographic features (such as size and shape descriptors, fabric and mineralogical indices) with a coefficient of determination equal to 0.87 which is not considered rock strength and hardness. Also, this model has more parameters for calculating.

Conclusions

In this research, the relation between CAI and engineering features was evaluated for 15 samples of 5 types of acidic igneous rocks extracted from the Gelas water transfer tunnel in west Azerbaijan (Naghadeh City) of Iran. Statically analysis, such as Pearson's correlation, simple and multiple linear and non-linear regression analysis has been performed to assess the relations between CAI and each engineering feature including texture coefficient (TC), heterogeneity (H), Saturation Index (SI), Feldspathic Index (FI), Uniaxial Compressive Strength (UCS), Abrasivity Index (ABI), and Rock Abrasivity Index (RAI). Based on Pearson's correlation analysis, the lowest correlation was between CAI and Sch, I_{S50}, and P in igneous rocks. The Uniaxial Compressive Strength (UCS) is the only mechanical property that shows a significant correlation with the Cerchar Abrasivity Index (CAI). As the CAI value increases, various engineering features including Texture Coefficient (TC), Heterogeneity (H), Saturation Index (SI), UCS, Abrasivity Index (ABI), and Rock Abrasivity Index (RAI) also increase. However, the Feldspathic Index (FI) and porosity (P) show a decreasing trend as the CAI value increases. CAI and TC have the best correlation in simple regression analysis (Table 8; Eq.15). In multiple linear regression analysis CAI, ABI, H, and SI revealed the highest correlation (Table 9; Eq.34). In multiple non-linear regression analysis CAI, ABI, H, and SI showed the highest correlation (Table 10; Eq.46). In ANN analysis CAI, ABI, H, and, SI are the best models (Table 11; Eq.58). The results of the analysis indicate that the Saturation Index (SI), Heterogeneity (H), and Abrasivity Index (ABI) are suitable parameters for comparing the abrasiveness of acidic igneous rocks. The study suggests that H is a better indicator than Texture Coefficient (TC), and the saturation index is more effective than the feldspathic index for comparing the Cerchar Abrasivity Index (CAI). These findings can be applied in predicting the wear of disc cutters used in Tunnel Boring Machines (TBMs) for this specific project involving acidic igneous rocks. However, it should be noted that the dataset used in this study was limited to acidic igneous rocks, and further validation is recommended for other rock types. The presented equations can serve as a starting point for future research in this field.

Funding

This study was funded by Vice-Chancellery for Research and Technology Affairs of Bu-Ali Sina University, Hamedan, Iran. The authors declare that no funds, grants, or other supports were received during the preparation of this manuscript.

Data Availability

No datasets were generated during the current study.

Competing Interests

The authors have no relevant financial or non-financial interests to disclose.

Conflict of Interest

The authors declare that they have no known competing financial interests or personal relationships that could have appeared to influence the work informed in this paper.

Authors' contributions

SSK: writing-original, draft-review, and editing; MH: supervisor and funding acquisition-review and editing; JKH: advisor and provided laboratory facilities- review and editing; MKE: perform tests, review, editing, and translation of article. EST: director of the project and provided useful information about the project, review and editing.

References

- Abu Bakar, M.Z., Majeed, Y., Rostami, J., 2016. Effects of rock water content on CERCHAR abrasivity index. Wear, 368-369:132-145.
- AFNOR. 2000. Determination du pouvoir abrasive d'une rochePartie 1: Essai de rayure avec une pointe (NF P 94-430-1) (In Paris).
- ANON. 1977. The Description of Rock Masses for Engineering Purposes. Engineering Group Working Party Report. Quaternary engineering geology, 10: 43-52.
- Alber, M., Yarali, O., Dahl, F., Bruland, A., Kasling, H., Michalakopoulos, T. N., Cardu, M., Hagan, P., Aydm, H., Ozarslan, A., 2014. ISRM suggested a method for determining the abrasivity of rock by the CERCHAR abrasivity test. Rock Mechanics and Rock Engineering, 47: 261-266.
- Aligholi, S., Lashkaripour, G.R., Ghafoori, M., 2018. Estimating engineering properties of igneous rocks using semi-automatic petrographic analysis. Bulletin of Engineering Geology and the Environment, 78: 2299-2314.
- Aydin, H., 2019. Investigating the effects of various testing parameters on Cerchar abrasivity index and its repeatability. Wear, 418-419: 61-74.
- Balani, A., Chakeri, H., Barzegari, G., Ozcelik, Y., 2017. Investigation of Various Parameters Effect on Cerchar Abrasivity Index with PFC3D Modeling. Geotechnical and Geological Engineering, 35: 2747–2762.
- Bieniawski, Z. T., 1975. The point load test in geotechnical practice. Engineering Geology, 11: 1-11. Er, S., Tugrul, A., 2016. Correlation of physicomechanical properties of granitic rocks with Cerchar Abrasivity Index in Turkey. Measurement, 91: 114-123.
- Ersoy, A., Waller, M. D., 1995. Textural characterization of rocks. Engineering Geology, 39: 123-136. Garzón-Roca, J., Torrijo, F. J., Alonso-Pandavenes, O., Alija, S., 2020. Cerchar Abrasivity Index Estimation of Andesitic Rocks in Ecuador from Petrographical Properties using Artificial Neural Networks. International Journal of Geomechanics, 20(5): 04020036. https://doi.org/10.1061/(ASCE)GM.1943-5622.0001632
- Ghasemi, A., 2010. Study of Cherchar abrasivity index and potential modifications for more consistent measurement of rock abrasion. Master of Science, the Pennsylvania State University, United States.
- Gharahbagh, E. A., Rostami, J., Ghasemi, A. R., Tonon, F., 2011. Review of rock abrasion testing. In: Proceeding of the 45th US Rock Mechanics/Geomechanics Symposium. San Francisco, California, June, 11-141.
- Hamzaban, M. T., Memarian, H., Rostami, J., Ghasemi-Monfared, H., 2014. Study of rock-pin interaction in Cerchar abrasivity test. International Journal of Rock Mechanics and Mining sciences, 72: 100-108. https://doi.org/10.1016/J.IJRMMS.2014.09.007
- Hassanpour, J., Rostami, J., Tarigh Azali, S., Zhao, J., 2014. Introduction of an empirical TBM cutter wear prediction model for pyroclastic and mafic igneous rocks; a case history of Karaj water

- conveyance tunnel Iran. Tunnelling and Underground Space Technology, 43: 222-231. https://doi.org/10.1016/j.tust.2014.05.007.
- Hassanpour, J., Esmaeili Vardanjani S., Cheshomi, A., Rostami, J., 2019. Engineering geological studies used for redesigning and employing a hard rock TBM in soft rock formations of Chamshir water conveyance tunnel, Geopersia, 9 (1): 1-20, (in Persian), DOI:10.22059/geope.2018.253479.648374
- Hecht-Nielsen, R., 1987. Kolmogorov's mapping neural network existence theorem. First IEEE International Conference on Neural Networks. San Diego, 11-14.
- Howarth, D. F., Rowlands, J. C., 1987. Quantitative assessment of rock texture and correlation with drillability and strength properties. Rock Mechanics and Rock Engineering, 20: 57-85. https://doi.org/10.1007/BF01019511
- ISRM, 2007. The Blue Book: The Complete ISRM Suggested Methods for Rock Characterization, Testing and Monitoring. 1974–2006. Compilation Arranged by the ISRM Turkish National Group, Ankara, Turkey.
- Johnson, R., 1998. Elementary statistics, 5th edn. PWS KENT Publishing Company. Boston.
- Karrari, S. S., Heidari, M., Khademi Hamidi, J., Sharifi Teshnizi, E., 2023. Predicting geomechanical, abrasivity, and drillability properties in some igneous rocks using fabric features and petrographic indexes. Bulletin of Engineering Geology and the Environment, 82: 124. https://doi.org/10.1007/s10064-023-03144-0
- Karrari, S. S., Heidari, M., Khademi Hamidi, J., Sharifi Teshnizi, E., 2024. New Cerchar Device Used for Evaluating Cerchar Abrasivity Parameters. International Journal of Geomechanics. 24(3), 04024005: 1-18. DOI: 10.1061/IJGNAI.GMENG-8676
- Khaleghi Esfahani, M., Kamani, M., Ajalloeian, R., 2019. An investigation of the general relationships between abrasion resistance of aggregates and rock aggregate properties. Bulletin of Engineering Geology and the Environment, 78: 3959-3968. https://doi.org/10.1007/s10064-018-1366-7
- Ko, T. Y., Kim, T. K., Son, Y., Jeon, S., 2016. Effect of geomechanical properties on Cerchar Abrasivity Index (CAI) and its application to TBM tunneling. Tunnelling and Underground Space Technology, 57: 99-111. http://dx.doi.org/10.1016/j.tust.2016.02.006
- Leys, C., Ley, C., Klein, O., Bernard, P., Licata, L., 2013. Detecting outliers: Do not use standard deviation around the mean, use absolute deviation around the median. Journal of Experimental Psychology, 49 (4): 764-766. DOI:10.1016/J.JESP.2013.03.013
- Lin, L., Xia, Y., Zhang, X., 2020. Wear Characteristics of TBM Disc Cutter Ring Sliding against Different Types of Rock. KSCE Journal of Civil Engineering, 24: 3145-3155. https://doi.org/10.1007/s12205-020-2208-2
- Majeed, Y., Abu Bakar, M. Z., 2015. Statistical evaluation of CERCHAR Abrasivity Index (CAI) measurement methods and dependence on petrographic and mechanical properties of selected rocks of Pakistan. Bulletin of Engineering Geology and the Environment, 75: 1341-1360. DOI 10.1007/s10064-015-0799-5
- Majeed, Y., Abu Bakar, M. Z., 2018. A study to correlate LCPC rock abrasivity test results with petrographic and geomechanical rock properties. Quarterly Journal of Engineering Geology and Hydrogeology, 51: 365-378. https://doi.org/10.1144/qjegh2017-112
- Massalov, T., Yagiz, S., Rostami, J., 2020. Relationship between Key Rock Properties and Cerchar Abrasivity Index for Estimation of Disc Cutter Wear Life in Rock Tunneling Applications. The ISRM International Symposium EUROCK 2020, physical event not held, ISRM-EUROCK-2020-162.
- McKenzie, J., 2011. Mean absolute percentage error and bias in economic forecasting. Economics Letters, 113 (3): 259-262. https://doi.org/10.1016/j.econlet.2011.08.010
- Mishra, D. A., Srigyan, M., Basu, A., Rokade, P. J., 2015. Soft computing methods for estimating the uniaxial compressive strength of intact rock from index tests. International Journal of Rock Mechanics and Mining sciences, 80: 418-424. https://doi.org/10.1016/j.ijrmms.2015.10.012
- Norusis, M., 2002. SPSS 11.0 Guide to data analysis. Prentice Hall Inc. Upper Saddle River.
- Omar, M., 2016. Empirical correlations for predicting strength properties of rocks-United Arab Emirates. International Journal of Geo-Engineering, 11 (3): 248-261.
- Ozturk, C. A., Nasuf, E., 2013. Strength classification of rock material based on textural properties. Tunnelling and Underground Space Technology, 37: 45-54.
- Ozturk, C. A., Nasuf, E., Kahraman, E., 2014. Estimation of rock strength from quantitative assessment of rock texture. Journal of the Southern African Institute of Mining and Metallurgy, 14(6): 471-480.

Peng, J., Wong, N. Y., The, C. I., 2017. Influence of grain size heterogeneity on strength and microcracking behavior of crystalline rocks. Journal of Geophysical Research: Solid Earth, 122: 1054-1073.

- Plinninger, R. J., 2002. Klassifizierung und Prognose von Werkzeugverschleiß bei konventionellen Gebirgslo "sungsverfahren im Statistical evaluation of CERCHAR Abrasivity Index's (CAI's) measurement methods and its...123 Festgestein." Mu "nchner Geologische Hefte, Reihe B-Angewandte Geologie, 17: 147.
- Plinninger, R. J., 2010. Hard rock abrasivity investigation using the Rock Abrasivity Index (RAI) Geologically Active. Taylor & Francis Group. London.
- Prikryl, R., 2006. Assessment of rock geomechanical quality by quantitative rock fabric coefficients: limitations and possible source of misinterpretations. Engineering Geology, 87: 149-162.
- Rostami, K., Khademi Hamidi, J., Nejati, H. R., 2020. Use of rock microscale properties for introducing a cuttability index in rock cutting with a chisel pick. Arabian Journal of Geosciences, 13: 960. https://doi.org/10.1007/s12517-020-05937-z
- Roy, L. B., 2017. Properties of rocks and their applications (Rock mechanics). Civil Engineering Department NIT Patna. Patna-800005.
- Schimazek, J., Knatz, H., 1970. the assessment of the cuttability of rocks by drag and roller bits. Ertz metal, 29: 113-119.
- Shi, X., Tang, Y., Chen, S., Gao, L., Wang, Y., 2024. Experimental study on the sandstone abrasiveness via mineral composition and microstructure analysis. Petroleum, 10: 440-445.
- Singh, T. N., Verma, A. K., 2012. Comparative analysis of intelligent algorithms to correlate strength and petrographic properties of some schistose rocks. Engineering with Computers, 28: 1-12.
- Streckeisen, A., 1976. To each plutonic rock its proper name. Earth Science Reviews. International Magazine for Geo-Scientists, Amsterdam, 12: 1-33.
- Teymen, A., 2020. The usability of Cerchar abrasivity index for the estimation of mechanical rock properties. International Journal of Rock Mechanics and Mining sciences, 128: 104258.
- Ticknor, J. L., 2013. A Bayesian regularized artificial neural network for stock market forecasting. Expert Systems with Applications, 40: 5501-5506.
- Torrijo, F. J., Garzón-Roca, J., Company, J., Cobos, G., 2020. Estimation of Cerchar abrasivity index of andesitic rocks in Ecuador from chemical compounds and petrographical properties using regression analyses. Bulletin of Engineering Geology and the Environment, 78: 2331-2344.
- Tumac, D., Copur, H., Balci, C., Er, S., Avunduk, E., 2017. Investigation into the Effects of Textural Properties on Cuttability Performance of a Chisel Tool. Rock Mechanics and Rock Engineering, 51: 1227-1248.
- Undul, O., Er, S., 2017. Investigating the effects of micro-texture and geo-mechanical properties on the abrasiveness of volcanic rocks. Engineering Geology, 229: 85-94.
- Verhoef, P. N. W., 1997. Wear of rock cutting tools (Implications for the site investigation of rock dredging projects). Balkema. 334.
- West, G., 1981. A Review of Rock abrasiveness testing for tunneling. In Proceedings of international symposium on weak rock. Tokyo, Japan, 585-594.
- West, G., 1989. Rock abrasiveness testing for tunneling. International journal of rock mechanics and mining sciences & Geomechanics abstracts, 26: 151-160.
- Yarali, O., Yasar, E., Bacak, G., Ranjith, P. G., 2008. A study of rock abrasivity and tool wear in coal measures rocks. International Journal of Coal Geology, 74: 53-66.
- Yarali, O., 2017. Investigation into Relationships between Cerchar Hardness Index and Some Mechanical Properties of Coal Measure Rocks. Geotechnical and Geological Engineering, 35: 1605-1614.
- Yagiz, S., Frough, O., Rostami, J., 2020. Evaluation of rock brittleness indices to estimate Cerchar Abrasivity Index for disc cutter weariness. The 54th U.S. Rock Mechanics/Geomechanics Symposium. Physical event cancelled. June. ARMA-2020-1805.



This article is an open-access article distributed under the terms and conditions of the Creative Commons Attribution (CC-BY) license.